THE ASTROPHYSICAL JOURNAL, 457:598–603, 1996 February 1

A DUST LANE IN THE RADIO GALAXY 3C 270

ASHISH MAHABAL AND AJIT KEMBHAVI
Inter-University Centre for Astronomy and Astrophysics, Post Bag 4, Ganeshkhind, Pune 411 007, India
K. P. SINGH AND P. N. BHAT
Tata Institute of Fundamental Research, Homi Bhabha Road, Bombay 400 005, India
AND
T. P. PRABHU
Indian Institute of Astrophysics, Bangalore 560 034, India
Received 1994 November 21; accepted 1995 July 18

ABSTRACT

We present broadband surface photometry of the radio galaxy 3C 270 (NGC 4261). We find a distinct dust lane in the $V-R$ image of the galaxy and determine its orientation and size. We use the major axis profile of the galaxy to estimate the optical depth of the dust lane, and discuss the significance of the lane to the shape of the galaxy.

Subject headings: dust, extinction — galaxies: individual (3C 270) — galaxies: photometry — radio continuum: galaxies

1. INTRODUCTION

3C 270 (NGC 4261) is a radio galaxy with a bright compact radio nucleus and prominent jets and lobes. While at first sight it appears to be a morphologically simple elliptical galaxy of type E2, closer examination reveals many interesting features. A dust lane roughly along the apparent major axis of the galaxy was reported by Mőllenhoff & Bender (1987), while others have failed to confirm its presence (e.g., Kormendy & Stauffer 1987; Peletier et al. 1990). On a much smaller angular scale, recent observations with the Planetary Camera on the *Hubble Space Telescope* (Jaffe et al. 1993) have led to the detection of an absorbing disk of radius $\sim 2 \times 10^{20}$ cm that is made up of cool dust and gas. The plane of the disk is nearly normal to the radio jets, which are oriented close to the apparent minor axis of the galaxy. Long-slit spectra (Davies & Birkinshaw 1986) have shown that the galaxy rotates around an apparent axis that lies only $6° \pm 4°$ from the apparent major axis, which suggests that the galaxy is prolate or close to prolate.

In this paper we use V and R images of NGC 4261 to confirm the existence of the dust lane first noted by Mőllenhoff & Bender (1987). We demonstrate the existence of the lane in the combined $V-R$ color image of the galaxy, determine its size and orientation, and estimate its optical depth from the color excess relative to the region immediately outside the dust lane. We then independently estimate the optical depth of the dust lane by examining the deviation of the surface brightness profile of the galaxy from de Vaucouleurs's law. We end with comments on the contribution of the dust lane to the observed boxiness of galaxy isophotes and the significance of the orientation of the lane to the radio structure and intrinsic shape of the galaxy.

2. OBSERVATION AND DATA REDUCTION

NGC 4261 was observed at the prime focus (f/3.5) of the 2.3 m Vainu Bappu Telescope at Kavalur on the night of 1992 March 3 as part of a program of broadband imaging of radio galaxies. The detector used was a Griboval electronographic camera (GEC) CCD with 576 × 385 pixels, each 22 × 22 μm^2 in size, corresponding to 0.56 × 0.56 arcsec^2 at the prime focus. We obtained two 600 s exposure frames in V and two 200 s frames in R, and a number of twilight sky flats and bias frames spread throughout the night. We observed standard stars in the *dipper asterism* region of the open cluster M67 for calibration; the procedure adopted has been described in detail by Anupama et al. (1994).

We followed the standard procedure for bias subtraction and flat fielding and performed sky subtraction for each frame using a mean sky value estimated from pixels in the four corners of the frame, all of which were unaffected by the galaxy. We combined the two frames in each filter into single V and R frames after performing translations and rotations so that the images were aligned to better than 0.1 pixel. Since the night was not photometric, we did not apply any extinction corrections. Tasks from IRAF[1] and STSDAS[2] were used for all the data reduction and analysis.

Boxiness is clearly discernible in the isophotes of NGC 4261, which nevertheless can be very well approximated by smooth ellipses. We fitted ellipses to the isophotes using routines in STSDAS, which are based on the method outlined by Jedrzejewski (1987). The semimajor axes of successive fitted ellipses were larger by a factor of 1.1, and the fit extended from the center to a semimajor axis length of 60″, where the error in the surface brightness reaches approximately 0.1 mag. The semimajor axis brightness profile, ellipticity, and position angle of the fitted ellipses as functions of semimajor axis length a for the V filter are shown in Figure 1. These parameters show similar behavior in R. The rather large error bars in case of ellipticity and position angle could be due to genuine departure of isophots from true ellipses. The deviation of an isophote from a perfect ellipse is estimated by expanding the difference in intensity between the isophote and the corresponding fitted ellipse as a Fourier series in the eccentric anomaly along the isophote.

[1] IRAF is distributed by the National Optical Astronomy Observatories, which is operated by the Association of Universities, Inc. (AURA), under cooperative agreement with the National Science Foundation.
[2] The Space Telescope Science Data Analysis System STSDAS is distributed by the Space Telescope Science Institute.

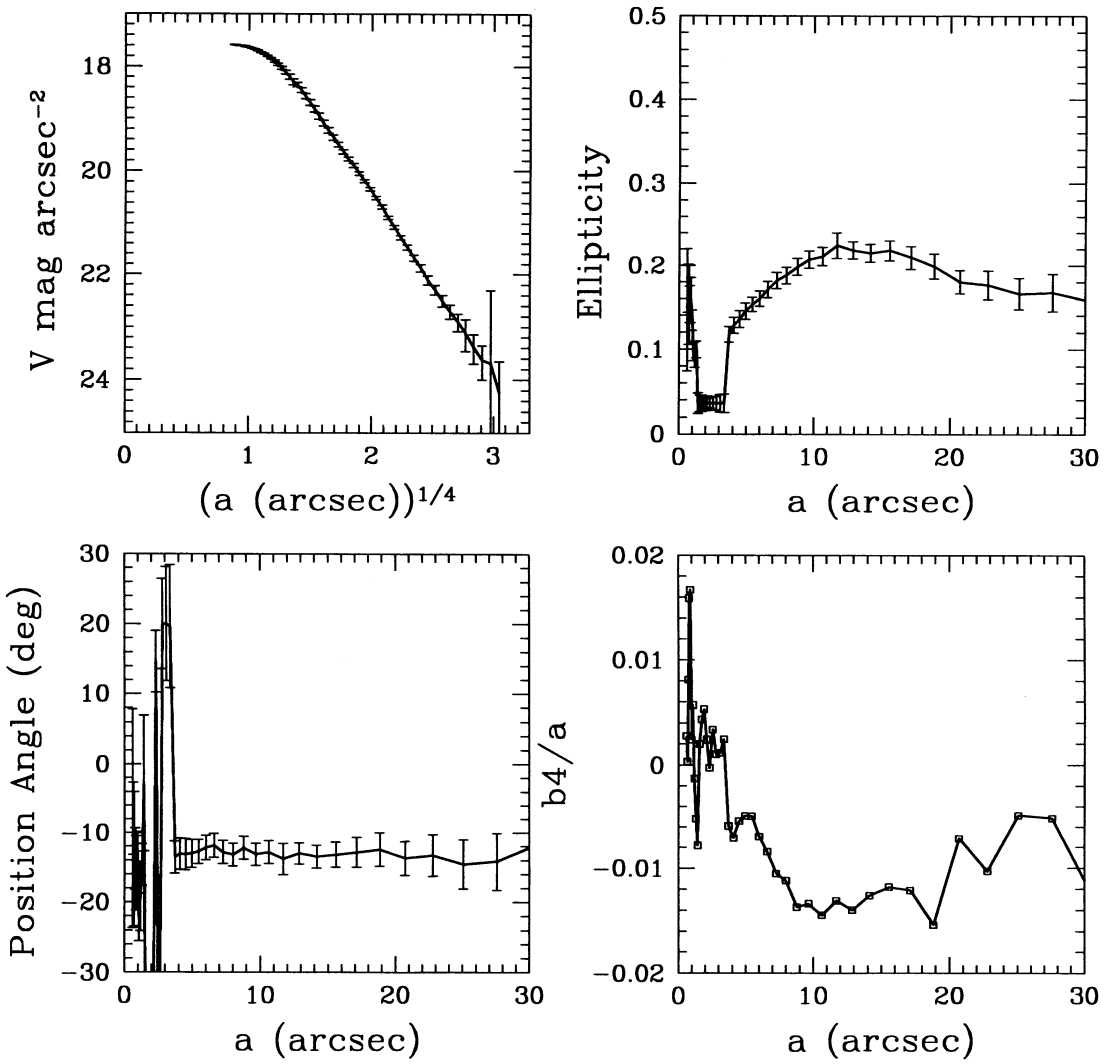

FIG. 1.—Semimajor axis profiles in the V band of surface brightness, ellipticity, position angle, and the *boxiness coefficient* $b4/a$. The surface brightness is shown as a function of $a^{1/4}$, where a is the semimajor axis length of the isophotes.

When boxiness is present, the coefficient $b4$ of the $\cos(4\phi)$ term is negative. We have shown in Figure 1 the ratio $b4/a$ as a function of a for images in the V filter. All the distributions in Figure 1 are in good agreement with the values obtained by Mőllenhoff & Bender (1987).

3. COLOR IMAGE

The putative dust lane in NGC 4261 is too faint to be seen in a single direct image, and the best place to look for it is a two-color image of the galaxy. Since we do not have a B frame with good signal-to-noise ratio, we investigate the $V-R$ image. The difference in the full width at half-maximum (FWHM) in the point-spread function (PSF) for the V and R images is $\sim 0''.06$, compared to the FWHM of $\sim 2''.4$. We therefore ignore the difference in further analysis. A narrow elongated structure is clearly seen in the $V-R$ image (Fig. 2 [Pl. 7]), oriented close to the apparent major axis of the galaxy. We show below that the feature is redder than its surroundings, and we interpret it as a dust lane. In order to improve the appearance of the lane, we have also constructed a modified color image adopting the procedure recommended by Sparks et al. (1985), which uses a smooth version of the higher wavelength image. This enhances the higher spatial frequency structures without affecting large-scale color features, and it reduces noise in the two-color image, as one of the components is smoothed. For this purpose we first fitted ellipses to the R image following the procedure described in the previous section, then obtained a smooth image $R_{\rm smooth}$ by interpolating between the isophotes using the ellipse parameters, and, finally, obtained the modified color image, $V-R_{\rm smooth}$, which is shown in Figure 3 (Plate 8). The elongated structure in the $V-R$ image is now more obvious than in Figure 2. The feature is also seen if the smooth image is obtained with the inclusion of higher harmonics that account for the boxiness of the isophotes. We wish to emphasize that all calculations presented in this paper are based on the original, unsmoothed V, R, and $V-R$ images.

A cut across the dust lane in the $V-R$ image, averaged over 10 rows around the galaxy center, is shown in Figure 4. Even though the instrumental color profile in the figure is noisy in the outer parts, it is clear that there is an overall shift to the blue as one moves toward the center of the galaxy. A region obviously more red in color than its immediate surroundings is seen straddling the center. The red color persists over the

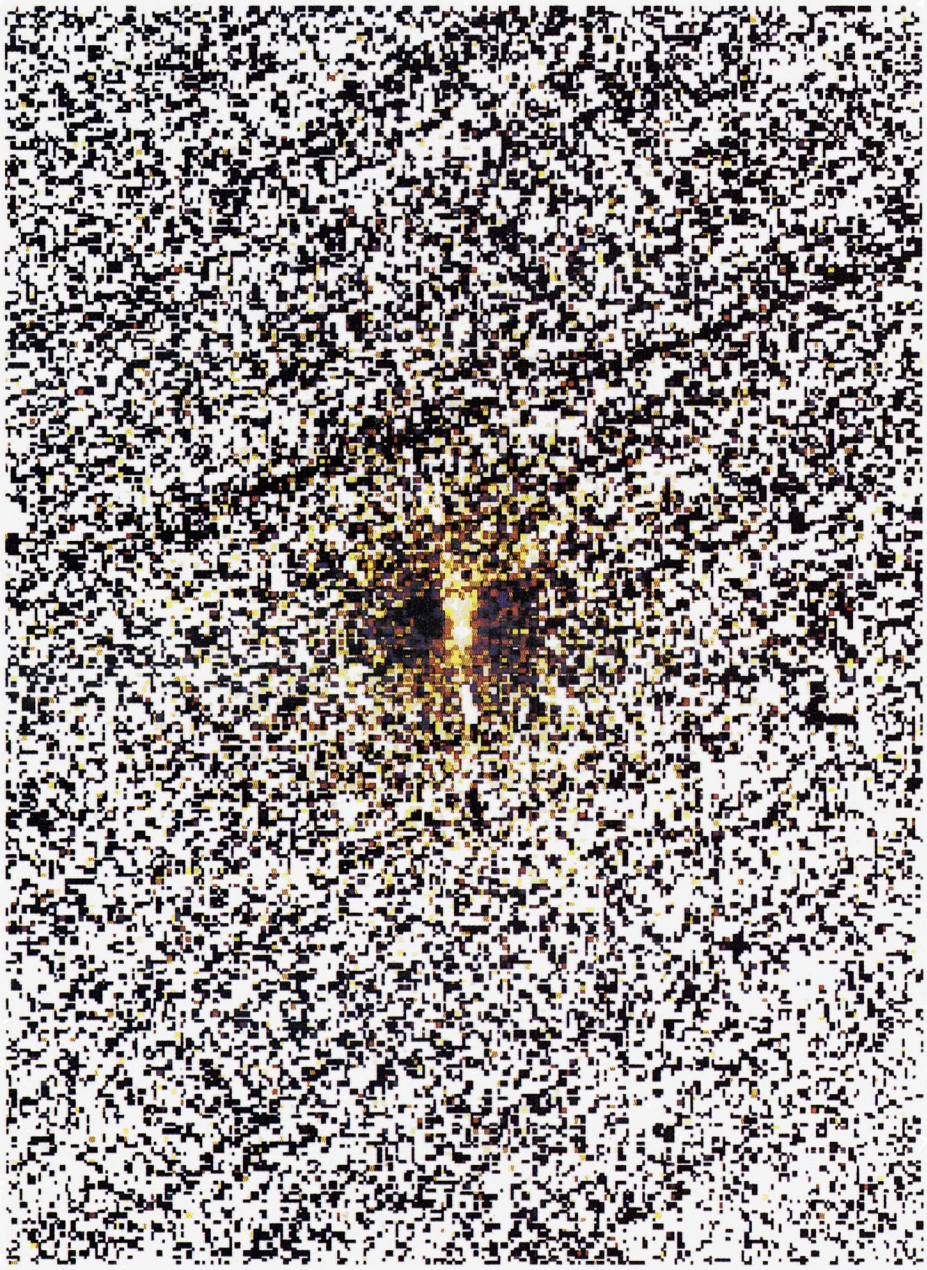

FIG. 2.—$V-R$ image of NGC 4261 in false color. Each pixel is 0.″56.

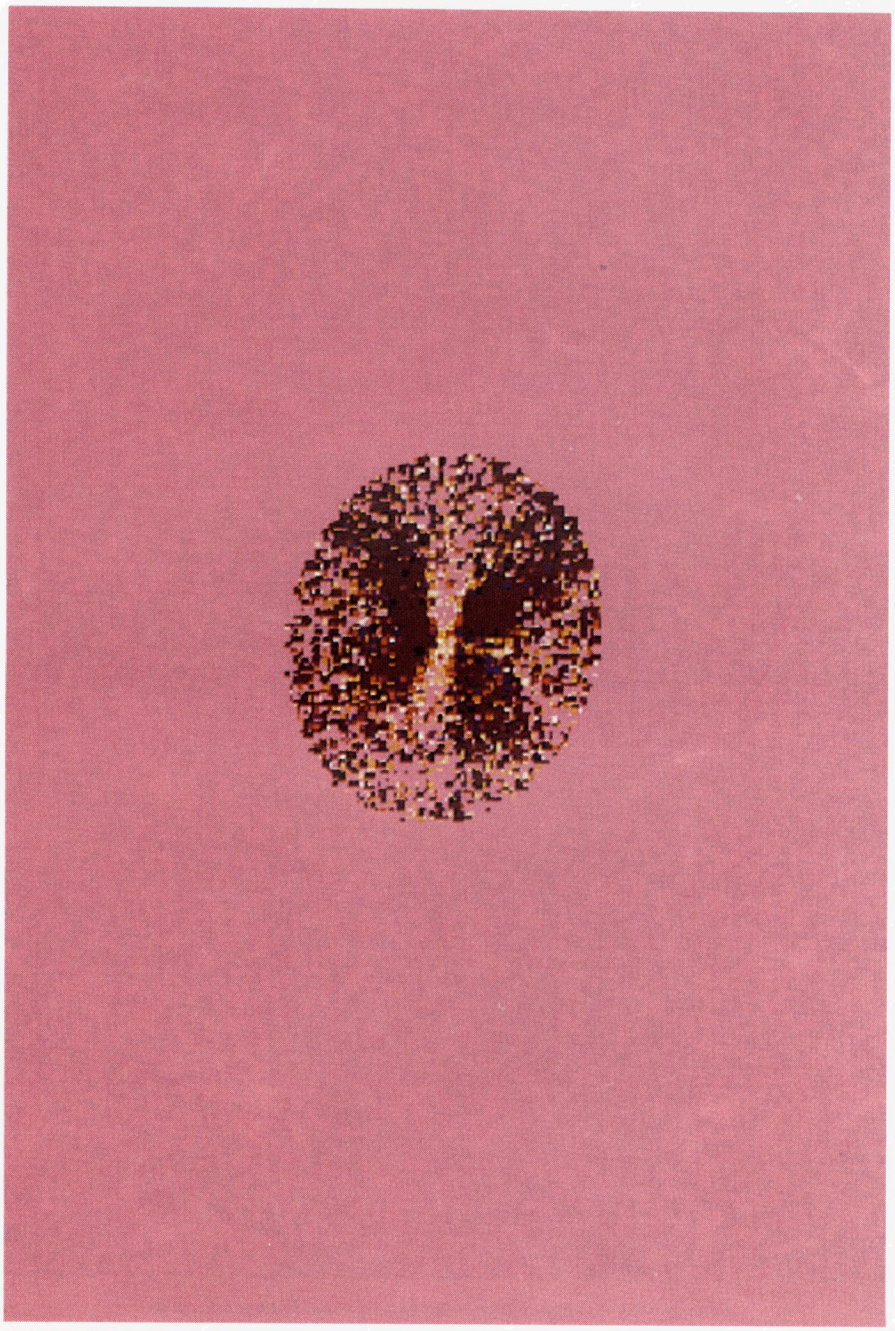

FIG. 3.—$V - R_{\rm smooth}$ image of NGC 4261 in false color. Each pixel is 0.″56.

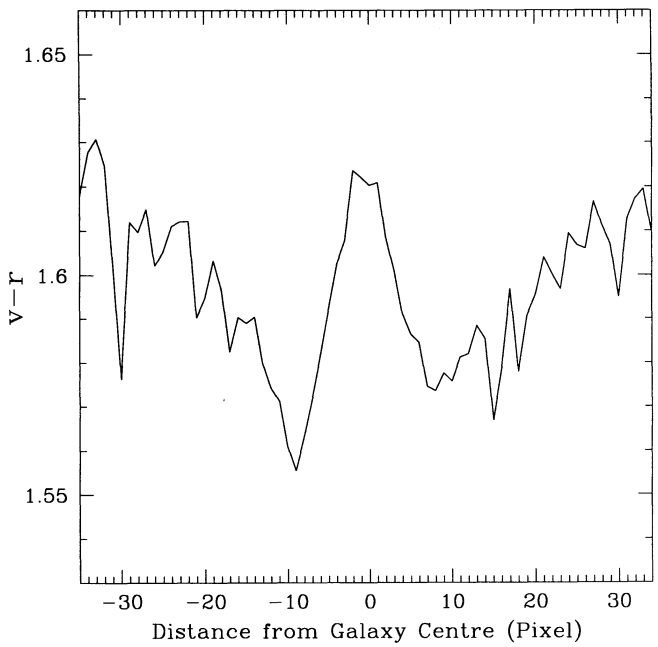

FIG. 4.—A cut across the dust lane, averaged over 10 rows around the galaxy center. The instrumental color $v - r$ is shown.

narrow feature, and we interpret it to be a thin disk of dust seen nearly edge-on and appearing as a dust lane.

From inspection of Figure 2, the extent of the dust lane is found to be approximately 21 × 6 arcsec^2. We have taken several 5 pixel wide cuts across the dust lane, and assuming that the maximum in the $V-R$ profile in such a strip corresponds to the center of the lane for that strip, we obtained the coordinates of the center along its length. A linear least-squares fit to these points then provides a straight-line representation of the dust lane. This is shown in Figure 5, along with the direction of the major axis obtained from the ellipse fits and the direction of the large-scale radio jet as given by Birkinshaw & Davies (1985). The dust lane makes an angle of 9° ± 1° with the major axis and an angle of 97° ± 1° with the radio jets.

We have estimated the color excess in the dust lane by comparing the color in it with that of the surroundings. For this purpose we used a circular aperture with radius 1.″68 (3 pixels) on the V and R frames separately to extract magnitudes along the lane and a region along the minor axis 10″ from the center, which is free of dust. The mean of the color excess obtained in this manner is

$$E(V-R) = (V-R)_{\rm dust} - (V-R)_{\rm galaxy} \simeq 0.05 \pm 0.01 .$$

Assuming that the composition of the dust in the disk is similar to that of dust in our galaxy, and using standard relations from Savage & Mathis (1979), it follows that $E(B-V) = 0.06$, $\tau_V = 0.17$, and $\tau_R = 0.08$, where τ is the optical depth. Because these numbers are small, the dust lane is not immediately apparent in the individual direct images. However, the dust does affect the luminosity profile, and we explore that aspect in the next section.

The optical depth obtained requires a correction since the dust disk obscures only those stars that are behind it and not the ones that are between the disk and the observer. It can be shown (Brosch et al. 1990) that if the fraction of stars obscured is f, then the relation between the observed extinction $A_\lambda^{\rm obs}$ and the optical depth τ_λ is

$$A_\lambda^{\rm obs} = -2.5 \log [1 + f(e^{-\tau_\lambda} - 1)] .$$

For $\tau_\lambda \ll 1$, the extinction is given by $A_\lambda^{\rm obs} \simeq 1.09 f \tau_\lambda$, which may be compared to the usual relation $A_\lambda \simeq 1.09\tau_\lambda$ obtained by assuming that all the stars are obscured. The value of f depends on the geometry and orientation of the disk. When the disk is inclined to the line of sight, as in the present case, it is expected that the near side of the disk is darker than the far side,[3] and this could be used to fix the inclination when better data is available.

Following Burstein & Heiles (1978), the column density of neutral hydrogen and the total neutral hydrogen content in the dust disk can be obtained from

$$N(H) = 5.8 \times 10^{21} E(B-V) \text{ atoms cm}^{-2} ,$$

$$N_{\rm tot}^{\rm H} = D^2 \int (\text{dust}) N(H) d\Omega .$$

Using $E(B-V) = 0.06$ and $D = 14.7$ Mpc, we get $N_{\rm tot}^{\rm H} = 1.8 \times 10^{63}$, i.e., $M_{\rm tot}^{\rm H} = 1.7 \times 10^6\ M_\odot$. H here refers to the neutral hydrogen. Assuming that the dust-to-gas mass ratio is approximately 10^{-2}, as in our Galaxy, we get the dust mass $M_d = 1.5 \times 10^4\ M_\odot$, which is a lower limit since a faint disk can extend beyond the confines currently detected. The factor f discussed above appears in the denominator of the integral defining $N_{\rm tot}^{\rm H}$. Therefore, since $f < 1$, the actual neutral hydrogen content is larger than the estimate.

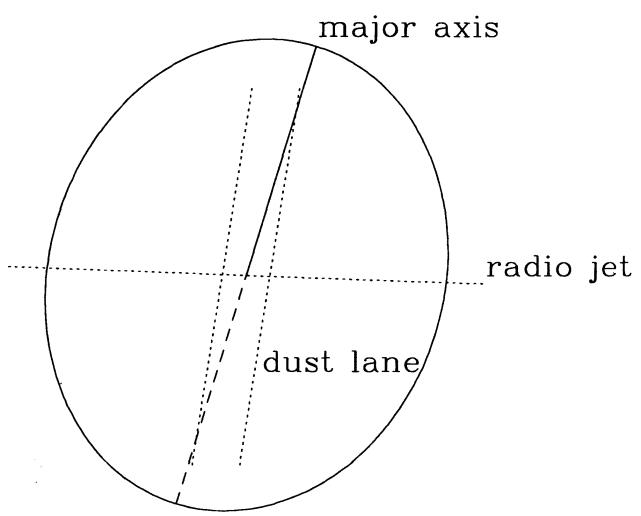

FIG. 5.—A schematic representation of NGC 4261. The major axis lies within the narrow confines of the dust lane, and the radio jet is almost perpendicular to it.

4. EFFECT OF DUST ON THE LUMINOSITY PROFILE

It is known that de Vaucouleurs's $r^{1/4}$ law describes very well the observed brightness distribution for elliptical galaxies within $0.1r_e \le a \le 1.5r_e$ (e.g., Burkert 1993), where a and r_e are the semimajor axis distance and effective radius, respectively. The lower limit is mainly due to seeing effects. Following an iterative fitting procedure, Burkert finds that for NGC 4261, $r_e = 34.''5$, so that de Vaucouleurs's law should hold at least up to ~3.″5. This procedure neglects the presence of the dust, which is expected to lead to departures from the law because of the absorption well above $0.1r_e$. The distribution of the surface

[3] We wish to thank an anonymous referee for pointing this out to us.

brightness of NGC 4261 as a function of $r^{1/4}$, where a is in arcsecond is shown in Figure 1. It is clear from the linear part of the curve for $a > 11''$ that de Vaucouleurs's law provides an excellent fit in this region. The departure from a straight line toward the center is due to seeing, absorption, and any real departures from the law at small radii.

We have fitted de Vaucouleurs's law to the V and R profiles after excluding the inner 11″. For the fit, a model galaxy was generated with assumed values of the effective radius r_e and central surface brightness and using the observed distribution of ellipticity. The model was convolved with the PSF obtained from stars in the frame, and the major axis profile was generated and compared with the observed profile. Parameters of the model were determined using the method of least squares. The effective radius obtained in this manner is 35″.8. The best-fit profile together with the observed surface brightness obtained from the ellipse fits described in § 2 is shown in Figure 6, and the agreement between the two in the region used in the fit is seen to be excellent. If all points of the observed profile are used in the fit, the effective radius r_e obtained is 42″.6, which is in agreement with the value obtained by Peletier et al. (1990) but is an overestimate because of the neglect of absorption.

The extrapolation of the best-fit profile to the region of the dust disk lies above the observed points. If this is attributed to the absorption due to dust, which is certainly valid for $a \geq 3''.5$, the difference ΔV in magnitude between the fit and the observed surface brightness directly provides a measure of the extinction, with optical depth $\tau_V = \Delta V/1.086$. The optical depth obtained in this manner for the V as well as the R filter is shown in Figure 7. There are two points to be noted here. (1) The optical depth is independent of any assumptions regarding the properties of the dust and therefore can be used to examine the validity of the assumptions made in § 3 in estimating optical depth from the color excess. (2) The observed surface brightness used in the determination of the extinction is obtained as a result of averaging over the best-fit ellipses, which improves the signal-to-noise ratio and provides a smooth representation of the dependence of the optical depth on the semimajor axis length.

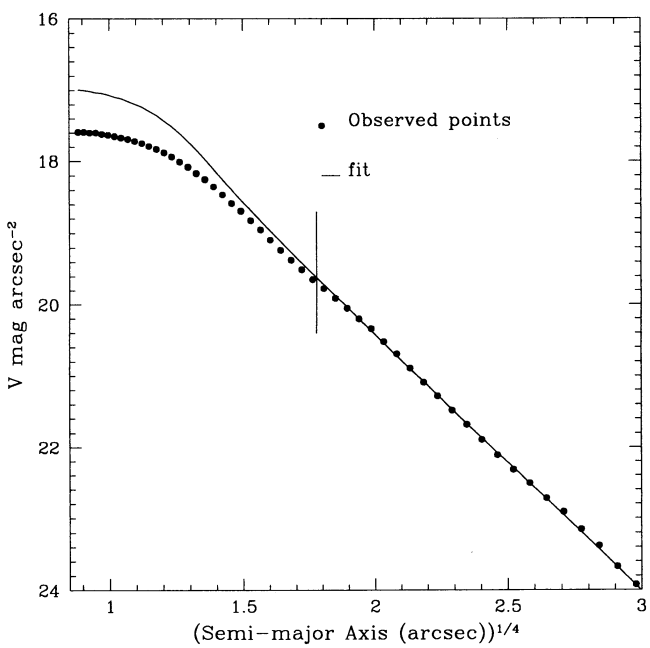

FIG. 6.—Observed brightness profile along the semimajor axis, and a de Vaucouleurs law fit made using points beyond the small vertical bar shown at $a = 11''$. The fit is extrapolated to the region inward of the bar. Deviation of the fit from the observed points in the inner region is indicative of the extinction due to dust.

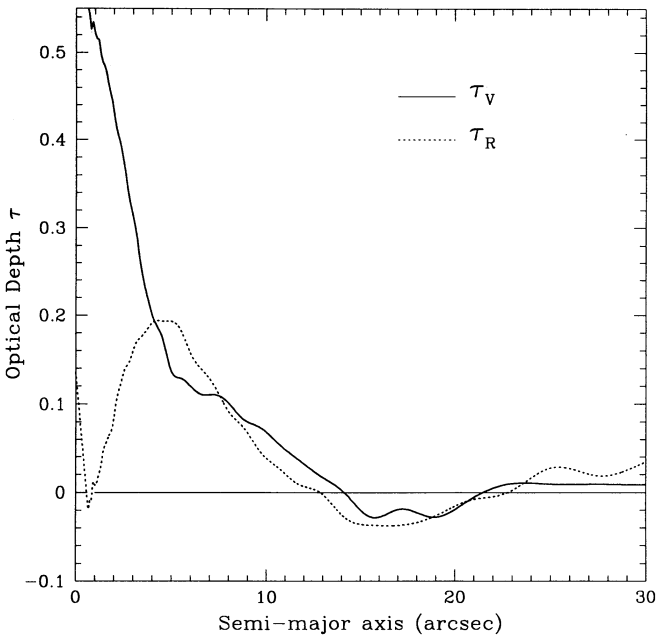

FIG. 7.—Optical depth τ_V and τ_R as function of a. The value at a given a is the mean over the best-fit ellipse with that semimajor axis.

For $8'' \leq a \leq 11''$ some points along the fitted ellipses lie outside the region covered by dust, and extinction obtained from the mean intensity as described above could be an underestimate. To check the magnitude of this effect, we have taken intensity cuts through the center that extended only through the region covered by dust. These were then averaged, and an intensity profile was obtained. We found that this profile differed at most by 0.01 mag from the profile obtained using the fitted ellipses. We therefore use the latter over the entire dust region.

The mean value of the optical depth over the dust region obtained using the above method separately for the two filters is $\tau_v = 0.19 \pm 0.01$ and $\tau_r = 0.10 \pm 0.01$, with the indicated error being primarily due to the uncertainty in deciding the extent of the dust-obscured region. The optical depth here agrees within errors with the value in § 3, which justifies the assumption made there that the dust in the disk is similar to the dust in our Galaxy.

It is possible to look for departures from the de Vaucouleurs law in the image rather than in the radial surface brightness profiles. For this purpose, using the best-fit de Vaucouleurs profile outside the putative dust region in the V filter, we have generated a two-dimensional model, extrapolated it to the region covered by the dust, and convolved the whole with the PSF. This provides a dust-free representation V_{df} of the galaxy. The residual image $V - V_{df}$ shows features similar to $V - R_{smooth}$, with some variations that arise because of the differences in model generation and smoothing used in the two cases. The similarity in the residual and color images makes it reasonable to assume that de Vaucouleurs's law modified by dust absorption provides a reasonable description of the inner region of NGC 4261.

It is expected that the optical depth in V is higher than that in R. However, in Figure 7 it is seen that $\tau_V \simeq \tau_R$ for $a \geq 4''$, and for $a < 4''$ there is decrease in optical depth τ_R while τ_V continues to rise. Literally taken, this would mean increased red light toward the center. Some elliptical galaxies are known to have red nuclei (e.g., Sparks et al. 1985) and red cores (e.g., Carter et al. 1983), but good spectroscopic data and observations in the B band under better seeing conditions will be necessary to confirm these trends here, as well as the similarity of the dust in NGC 4261 and in our Galaxy. Dust in the two galaxies could have significantly different properties because of different origins and environments. The active galactic nucleus in the radio galaxy could also have some effect on the dust (Begelman 1985; Shanbhag & Kembhavi 1988). The results at small radii would of course be affected by any color-dependent departures from de Vaucouleurs's law.

5. DUST AND ISOPHOTE BOXINESS

The dust lane reduces the surface brightness at every point along its extent, which results in the isophotes appearing to be pulled inward. When the dust lane is oriented along the major axis, this produces the appearance of boxiness, with the coefficient $b4$ of the cos (4ϕ) term in the angular dependence of the differential intensity along the best-fit ellipses becoming negative. To examine the magnitude of this effect, we have generated an elliptical galaxy with the central surface brightness and effective radius obtained for the best-fit model in § 3, using tasks from IRAF that allow the introduction of Poisson shot noise and characteristics of the CCD. After convolving the model with the observed PSF, we have placed in it a dust lane that has the extent and optical depth observed in NGC 4261 in the V band. We have then fitted ellipses to the isophotes and obtained $b4/a$, which is shown in Figure 8. The magnitude of $b4/a$ is seen to be similar to the observed value where dust is present, and the circularizing effect of the seeing is not dominant. However, the boxiness is color dependent, unlike in the observed case, and reduces to insignificant values as soon as the dust is left behind. Nevertheless, it is clear that observed isophotal boxiness could have a contribution from dust and could in fact be used as a diagnostic of major axis dust lanes that are too faint to be seen directly. In the same manner, dust lanes oriented in directions other than the apparent major axis will produce changes in isophotal shape that can be traced in the various Fourier coefficients.

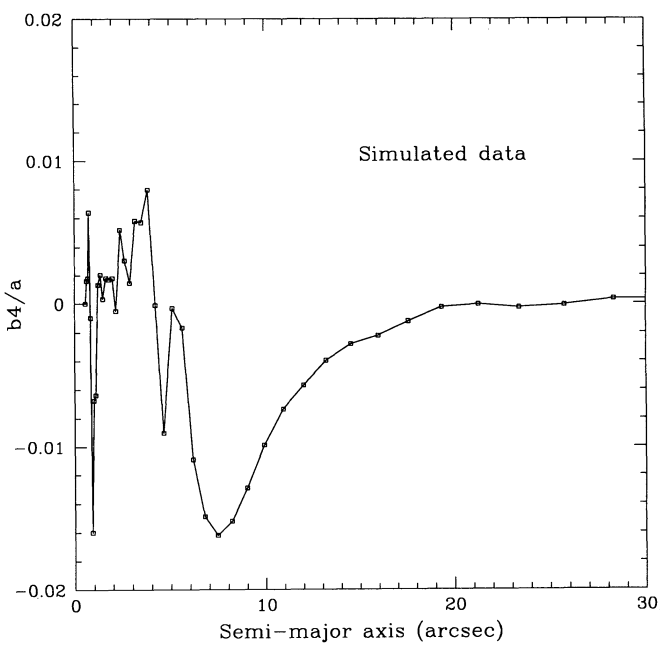

FIG. 8.—The *boxiness coefficient* for a simulated elliptical galaxy generated using the parameters obtained for NGC 4261.

6. DISCUSSION

The shape and orientation of a dust disk in an elliptical galaxy is determined by the allowed trajectories of the dust particles, which depend on the shape and the overall rotation of the galaxy. NGC 4261 shows rotation around the apparent major axis (Davies & Birkinshaw 1986) and therefore it cannot be an oblate spheroid (Binney 1985). Davies and Birkinshaw have argued from the kinematical data and modeling that the galaxy is prolate or triaxial and nearly prolate. In such a configuration, orbits in the equatorial plane (which is normal to the long axis) are stable, but these are not appropriate to describe the dust disk in NGC 4261, because the dust lane is observed to be aligned close to the major axis. However, there is another class of orbits that is stable (see Kormendy & Djorgovoski 1989 and de Zeeuw & Franx 1991 for a review of the possibilities and references) and has different orientations at different radii, which may be more appropriate to the present case. At small radii these orbits are polar, i.e., they lie in a plane containing the long and short axes; at larger radii the orbits are equatorial and skew at intermediate radii. The small-scale absorption disk discovered using the *Hubble Space Telescope* (Jaffe et al. 1993) is inclined at an angle of approximately 64° to the plane of the sky, while the inclination of the larger disk is approximately 75°. The two disks are to be viewed as the warped parts of a single disk, with the warping being due to the complex nature of the orbits and the possible change in the shape of the galaxy from prolate to oblate toward the inner region, which will change the plane of stable orbits. The relative orientation of the different parts of the disk is also dependent on the extent to which the parts have settled in their final orbits, and projection effects that again depend on the shape of the galaxy and the direction of the line of sight. Higher signal-to-noise ratio observations under better seeing conditions as well as spectroscopic data will be able to provide further information about the extent and shape of the dust disk that can be used in modeling the galaxy.

The radio jet in NGC 4261 is oriented almost normal to the dust disk, which hints at a possible connection between the two. The direction of the angular momentum of the disk changes somewhat from region to region as the disk is warped. It would be reasonable for the direction of the base of the jet to be determined by the innermost parts of the disk, and precession of the disk would lead to a change in the direction of the jet. However, the large-scale jet may overall appear to be normal to the large-scale disk. Based on the statistical analysis of radio jet directions (e.g., Palimaka et al. 1979; Kapahi & Saikia 1982), it has been argued that the jets are oriented along the apparent minor axis of elliptical galaxies. When the galaxy is an oblate spheroid, the apparent minor axis always coincides with the projection of the short axis. The observation then means that jets are preferentially emitted close to the short axis. This coincidence could be related to the fact that in nonrotating or slowly rotating oblate spheroids the equatorial plane has stable orbits, so that the accretion disk is situated in

this plane or close to it. When the galaxy is prolate, triaxial, or rotating, the situation is more complex, and, as mentioned above, a variety of stable orbits is possible. If the jet direction is again taken to be determined by a disk, the relation between the jet direction and the apparent minor axis will depend on the shape of the galaxy, the initial conditions of dust formation, and the viewing direction. One should also expect to find a disk at least in those ellipticals that are powerful radio galaxies with well-collimated jets. As in the case of NGC 4261, these disks may be too faint to be observed directly, but it would not be difficult to spot them using the techniques we have discussed above. If elliptical galaxies are the results of mergers or cannibalism, one may well find dust disks in all of them.

7. CONCLUSIONS

The main conclusions of the present paper are the following.

1. The radio galaxy NGC 4261 contains a dust lane with dimensions approximately 21 × 6 arcsec^2, oriented close to the apparent major axis of the galaxy. The dust lane can be interpreted as the projection of a dust disk with inclination angle approximately 75° to the plane of the sky. The observed color excess is $E(V-R) = 0.05$. Assuming dust properties similar to those in our galaxy, the optical depth obtained from $A_\lambda \simeq 1.09\tau_\lambda$ is $\tau_V = 0.17$ and $\tau_R = 0.08$. The actual optical depth could be a factor of about 2 higher than this value.

2. The optical depth can be estimated directly from departures of the surface brightness profile from de Vaucouleurs's law, and it has values close to those obtained from the color excess, confirming that the dust is similar to that in our Galaxy.

3. Absorption due to a major axis dust lane can produce boxiness that is color dependent.

The authors wish to thank the staff of the Vainu Bappu Observatory, Kavalur, for help with the observations, and Professors D. Lynden-Bell, G. C. Anupama, and S. K. Pandey for many enlightening discussions.

REFERENCES

Anupama, G. C., Kembhavi, A. K., Prabhu, T. P., Singh, K. P., & Bhat, P. N. 1994, A&AS, 103, 315
Begelman, M. C. 1985, ApJ, 279, 492
Binney, J. 1985, MNRAS, 212, 767
Birkinshaw, M., & Davies, R. L. 1985, ApJ, 291, 32
Brosch, K., Almoznino, E., Grosbol, P., & Greenberg, J. M. 1990, A&A, 233, 341
Burkert, A. 1993, A&A, 278, 23
Burstein, D., & Heiles, C. 1978, ApJ, 225, 40
Carter, D., Jorden, P. R., Thorne, D. J., Wall, J. V., & Straede, J. C. 1983, MNRAS, 205, 377
Davies, R. L., & Birkinshaw, M. 1986, ApJ, 303, L45
de Zeeuw, T., & Franx, M. 1991, ARA&A, 29, 239
Jaffe, W., Ford, H. C., Ferrarese, L., van den Bosch, F., & O'Connell, R. W. 1993, Nature, 364, 213
Jedrzejewski, R. 1987, MNRAS, 226, 747
Kapahi, V. K., & Saikia, D. J. 1982, J. Astrophys. Astron., 3, 161
Kormendy, J., & Djorgovski, S. 1989, ARA&A, 27, 235
Kormendy, J., & Stauffer, J. 1987, in IAU Symp. 127, Structure and Dynamics of Elliptical Galaxies, ed. T. de Zeeuw (Dordrecht: Reidel), 405
Mőllenhoff, C., & Bender, R. 1987, A&A, 174, 63
Palimaka, J. J., Bridle, A. H., Fomalont, E. B., & Brandie, G. W. 1979, ApJ, 231, L7
Peletier, R., Davies, R. L., Illingworth, G. D., Davis, L. E., & Cawson, M. 1990, AJ, 100 (4), 1091
Savage, B. D., & Mathis, J. S. 1979, ARA&A, 17, 73
Shanbhag, S., & Kembhavi, A. K. 1988, ApJ, 334, 34
Sparks, W. B., Wall, J. V., Thorne, D. J., Jorden, P. R., van Breda, I. G., Rudd, P. J., & Jorgensen, H. E. 1985, MNRAS, 217, 87